

Parallel and Perpendicular Susceptibility Above T_c in $\text{La}_{2-x}\text{Sr}_x\text{CuO}_4$ Single Crystals

Gil Drachuck,¹ Meni Shay,^{1,2} Galina Bazalitsky,¹ Jorge Berger,² and Amit Keren¹

¹*Department of Physics, Technion - Israel Institute of Technology, Haifa, 32000, Israel*

²*Physics Unit, Ort Braude College, P.O. Box 78, 21982 Karmiel, Israel*

(Dated: April 6, 2022)

We report direction-dependent susceptibility and resistivity measurements on $\text{La}_{2-x}\text{Sr}_x\text{CuO}_4$ single crystals. These crystals have rectangular needle-like shapes with the crystallographic “c” direction parallel or perpendicular to the needle axis, which, in turn, is in the applied field direction. At optimal doping we find finite diamagnetic susceptibility above T_c only when the field is perpendicular to the planes. In an underdoped sample there is finite diamagnetic susceptibility above T_c in both field directions. The variations in the susceptibility data suggests a different origin for the fluctuating superconductivity above T_c between under and optimal doping.

The superconducting and ferromagnetic phase transitions share a lot in common, but it is simpler to visualize the order parameter of the latter. A ferromagnet produces a magnetic field only if all its domains are aligned. Similarly, a superconductor has no resistance only if the phase of the order parameter is correlated across the entire sample. However, there are temperatures high enough so that a ferromagnet has local magnetization, but without global alignment. Similarly, a superconductor can have local diamagnetism, without zero resistance across the sample. This situation is the hallmark of fluctuating superconductivity without global phase coherence. In a two dimensional system, where long range order is forbidden [1], the role of domains is played by a vortex anti vortex pair, which break the fabric of the phase.

In the highly anisotropic cuprates superconductors, the presence of diamagnetism well above the resistance critical temperature, T_c , was demonstrated some time ago, with high magnetic field H perpendicular to the superconducting planes [2]. This finding was, indeed, interpreted as persistence of finite order parameter amplitude throughout the sample, but with short-range phase coherence above T_c . However, a completely different interpretations could be offered to the same effect, in which electrons are inhomogeneously localized due to the randomness of the dopant. There are several experimental indication for inhomogeneously localization [3]. In this case superconductivity can occurs with finite order parameter amplitude only in three dimensional patches of the sample, leading to local diamagnetic signal without a continues resistance-free path at $T > T_c$. In the localization scenario, diamagnetic signal should be detected above T_c for all directions of the applied field H .

In this work, we examine the fluctuating superconductivity using magnetization (M) measurements of $\text{La}_{2-x}\text{Sr}_x\text{CuO}_4$ with the field parallel and perpendicular to the CuO_2 planes. We work in the zero field limit, as required from the definition of susceptibility. We also perform resistivity measurements on the exact same samples. Our major finding is a diamagnetic signal in the resistive phase of highly underdoped sample, for both par-

allel and perpendicular field supporting the localization scenario.

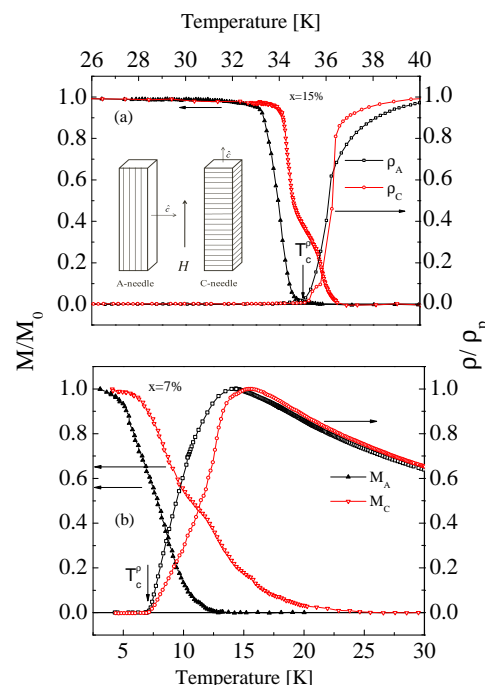


FIG. 1: LSCO normalized magnetization (left axis) and resistivity (right axis) measurements as a function of temperature of (a) optimally doped ($x = 15\%$) and (b) underdoped ($x = 7\%$) samples in an applied field of $H = 0.5$ Oe for two types of samples: A- and C-needs. In these needles the superconducting planes are parallel or perpendicular to the needle symmetry axis respectively. The magnetic field is applied along the needles. The A-needle is $1 \times 1 \times 10$ mm³ and the C-needle is $1 \times 1 \times 5$ mm³. M_0 is the magnetization at zero temperature and ρ_p is the resistivity at the peak. T_c^p indicates zero resistivity.

In magnetization experiments in the zero field limit, the measured susceptibility $\chi_m = \lim_{H \rightarrow 0} M/H$ depends on the sample geometry via the demagnetization factor (D), and is given by $\chi_m = \chi_i/(1 + D\chi_i)$ where χ_i is the intrinsic susceptibility. For needle-like samples, $D \simeq 0$

and $\chi_m = \chi_i$. Therefore, in order to determine χ_i properly needle-like samples are needed. To achieve the $D \simeq 0$ condition we use rod-like $\text{La}_{2-x}\text{Sr}_x\text{CuO}_4$ single crystals grown in an image furnace, which are oriented with a Laue camera and a goniometer. After the orientation, the goniometer with the rod is placed on a saw to cut the needles. Two configurations are cut as shown in Fig. 1. These crystals have rectangular needle-like shapes with the crystallographic “c” direction parallel or perpendicular to the needle axis. We were able to prepare 10 mm long A-needles and only 5 mm long C-needles. The field is applied also in the needle axis direction. For each sample we performed direction-dependent susceptibility and resistivity measurements. The measurements are done in zero field cooling conditions using a Cryogenic SQUID magnetometer equipped with a low field power supply with a field resolution of 0.01G. Prior to each measurement batch, the external field is zeroed with a Type I SC. After the measurement, the needles were chopped and T_c of each piece was tested to insure uniform T_c (see supplementary material).

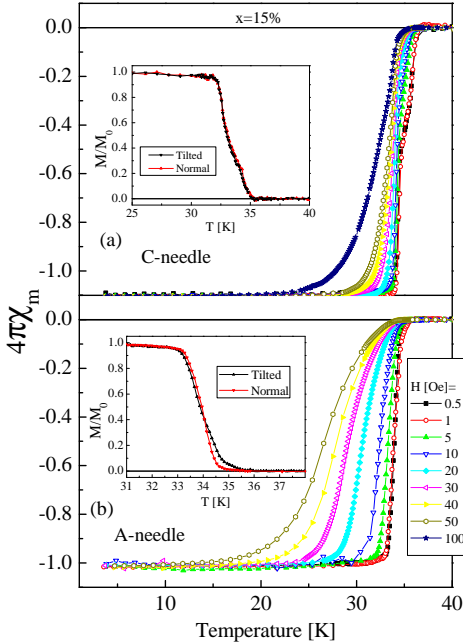


FIG. 2: The measured susceptibility χ_m ($\equiv M/H$) as a function of temperature for the 15% (a) C-needle and (b) A-needle in various magnetic fields. Insets: measurements of a straight and tilted needles demonstrating the effect of misalignment.

Figure 1(a) and (b) demonstrates our major finding. In this figure we depict the normalized magnetization M/M_0 as a function of T , at a field of $H = 0.5$ Oe, for the $x = 15\%$ and 7% samples respectively, for two different orientations. M_A and M_C are measurements performed on the A- and C-needle respectively. M_C shows

a knee just when M_A becomes finite. Resistivity data, normalized to 1 at the peak, are also presented in this figure; ρ_A and ρ_C are the resistivities measured with the corresponding needles with the contacts along the needles. The resistivity results are similar to those previously reported [4]. There is no observable difference in the critical temperatures defined as zero resistivity $[T_c^p]$ as determined by ρ_A or ρ_C . In contrast, there is a clear anisotropy in the temperature at which the magnetization is detectable; this difference increases as the doping decreases. For the 15% sample: M_A is not detectable above $T_c^p = 35$ K, but M_C is finite up to 36.5 K. The critical temperature of the material T_c , could be defined by either T_c^p or by the presence of three dimensional diamagnetism (finite M_A). The strong residual M_C above T_c^p without residual M_A was never detected before in such low fields. It could result from decoupled superconducting planes disordered by vortices.

In contrast, for the 7% case, both M_A and M_C are finite at temperatures well above $T_c^p = 7.0$ K. M_A is not detectable only above 13 K and M_C is finite up to 25 K. The sharpest transition is observed with the M_A measurement and this type of measurement could be used to define doping and sample quality. The dramatic difference between the 15% and 7% doping indicates that the fluctuating superconductivity above T_c^p at low doping is fundamentally different from optimal doping, and could be derived by electronic inhomogeneous localization.

In order to verify these results we performed several control experiments. First we examine the influence of the field on the susceptibility. In Fig. 2 (a) and (b) we plot $4\pi\chi_m$ for the 15% C- and A-needles respectively, as a function of temperatures, and for several applied magnetic fields. For the field range presented, the saturation value of the susceptibility is field-independent. At $T \rightarrow 0$, $4\pi\chi_m = -1.1$ and -1.05 for the C- and A-needles respectively. For our rectangular C-needle, with dimensions of $1 \times 1 \times 5$ mm³, the demagnetization factor is $D \simeq 4\pi \times 0.09$, which explains well the measured susceptibility. For our rectangular A-needle with dimensions of $1 \times 1 \times 10$ mm³, $D \simeq 4\pi \times 0.045$ and we expect $4\pi\chi_m = -1.05$, which is slightly higher than the observed value [5]. A more accurate analysis of the susceptibility of needles is given below. At the other extreme, when $T \rightarrow T_c$ we see field-dependent susceptibilities but only for fields higher than 1 Oe. Below 1 Oe, $\chi_m(T)$ converges to a field-independent function representing the zero field susceptibility. Therefore, all our measurements are done with a field of 0.5 Oe. Finally, the knee exists in the $M_C(T)$ data only for fields lower than 10 Oe. Similar data for 7% is given in the supplementary material.

We also examined the relevance of misalignment of the samples to our results by purposely introducing a tilt of 7° to the 15% needles. The measurements of a straight sample and a tilted one are shown in the insets of Fig. 2. Tilt measurements for the 7% needles are given in the

supplementary material. Misalignment can lead to an error of 0.1 K per 1° in the estimate of the temperature at which the magnetization is null. This tiny effect cannot account for the difference in the magnetization between the A- and C-needles. In addition, the tilt make no different to the presence of the knee.

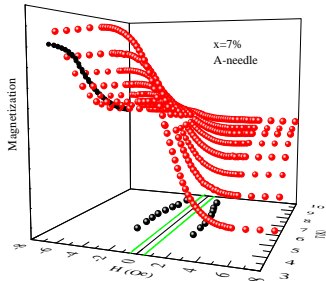


FIG. 3: A 3D plot of the magnetization as a function of magnetic field and temperature for the 7% A-needle. (floor): H_{c1} as a function of temperature. (wall): Magnetization as a function of T . The green solid line on the floor represents the applied field used in Fig. 1

Another concern is vortices. At a certain temperature close to T_c , the critical field H_{c1} must drop below the applied magnetic field and vortices can enter the sample. This puts a limit on the range of temperature where interpretation of our data is simple. Therefore, it is important to understand the behavior of H_{c1} near T_c . Figure 3 shows the results of $M(H, T)$ for $x = 7\%$ A-needle using a 3D plot. The values of H_{c1} are determined by fitting $M(H)$ to a straight line around $H = 0$ (not shown), and extracting the field where linearity breaks. $H_{c1}(T)$ is shown on the floor of the plot. The applied field, depicted as the straight green line on the floor, is lower than H_{c1} up to 12 K. At higher temperatures vortices can enter the sample.

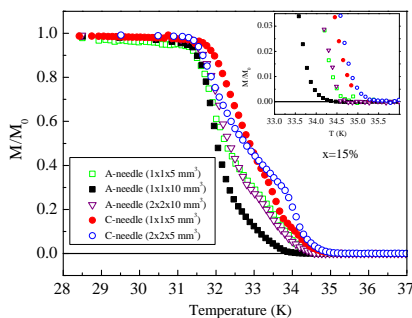


FIG. 4: Magnetization versus temperature for several 15% A- and C-needles with different sample dimensions. Inset: A zoom-in close to the transition temperature.

We also measured H_{c1} for the other samples (supplementary material). In particular, a field of $H = 0.5$ Oe is lower than H_{c1} for the 7% C-needle up to 20 K. This finding rules out the possibility that the knee observed in our C-needle measurements at fields lower than 10 Oe are due to lock-in/unlock-in transition of flux lines [6]. The knees of the 7% C-needle occurs at temperatures of 15 K at which the applied field is well below H_{c1} and no vortices exist in the sample. On the other hand, it is conceivable that the knee is a result of a transition between coupled and decoupled CuO_2 planes.

Finally, we investigated the impact of the sample geometry on the magnetization. The motivation here was to change the dimensions of the needles in terms of length-to-width ratio while maintaining needle-like aspect ratio. In Fig. 4 we present a multitude of 15% measurements for A- and C-needles. Similar data for the 7% samples are given in the supplementary material. The inset is a zoom close to T_c . The details of the magnetization curve are shape-dependent. However, the $2 \times 2 \times 10 \text{ mm}^3$ and $1 \times 1 \times 5 \text{ mm}^3$ A-needles have the same curve, demonstrating that the length-to-width ratio is the most important parameter. The closer the samples are to the ideal needle-like conditions, the bigger the difference in the magnetization between the two directions. This is, of course, expected since for a cubic or a spherical geometry, field lines cross the planes at an angle thus mixing the two susceptibilities leading to indistinguishable susceptibilities close to T_c [7].

All these tests support our observation that the magnetization of the A- and C-needle are fundamentally different by an amount larger than any possible experimental error. One might try to explain these differences as a finite size effect, namely, as the penetration depth diverges as $T \rightarrow T_c$ it might have a different values for each of the two different directions. Our magnetometer picks up a diamagnetic signal only when the penetration depth is similar to the sample width. This could occur at different temperatures, which are also different from T_c^o .

To address this possibility, we examined the London penetration depth (λ) in our 7% sample. In C-needle measurements, the screening currents run in the ab planes and the susceptibility is sensitive to the in-plane penetration depth λ_{ab} . In contrast, in the A-needle measurements, the screening currents run both in the plane and between planes. Therefore, the susceptibility is sensitive to both λ_{ab} and the penetration length between planes λ_c . To extract these λ 's we solve an anisotropic London equation

$$b_A - \lambda_{ab}^2 \frac{\partial^2 b_A}{\partial x^2} - \lambda_c^2 \frac{\partial^2 b_A}{\partial y^2} = 0 \quad (1)$$

$$b_C - \lambda_{ab}^2 \frac{\partial^2 b_C}{\partial x^2} - \lambda_{ab}^2 \frac{\partial^2 b_C}{\partial y^2} = 0 \quad (2)$$

with the boundary condition $b_\alpha = 1$, where b_A and b_C are the internal field divided by the applied field in the A- and C-needles respectively [8]. We define $\langle b_\alpha \rangle$ as the cross section average of b_α . For the A-needle we find

$$\langle b_A \rangle = \sum_{n \text{ odd}}^{\infty} \left\{ \frac{2/\sinh(\beta_n g) - 2/\tanh(\beta_n g) + \beta_n g}{gj^2 \beta_n^3/8} (3) + \frac{2/\sinh(\mu_n j) - 2/\tanh(\mu_n j) + \mu_n j}{jg^2 \mu_n^3/8} \right\}$$

where $g = w_y/\lambda_c$, $j = w_x/\lambda_{ab}$, $\beta_n = \sqrt{\left(\frac{\pi n}{j}\right)^2 + 1}$,

$\mu_n = \sqrt{\left(\frac{\pi n}{g}\right)^2 + 1}$, and w_x/w_y is the sample width taken as 1 mm. $\langle b_C \rangle$ is obtained from Eq. 3 by $\lambda_c \rightarrow \lambda_{ab}$. The susceptibility is given by $\chi_\alpha = (\langle b_\alpha \rangle - 1)/4\pi$. This provides an analytical solution for $\chi_C(\lambda_{ab})$ and $\chi_A(\lambda_{ab}, \lambda_c)$.

We obtain λ_{ab} by equating the analytical solution to the measured susceptibility of the C-needle. We then substitute this λ_{ab} into χ_A and extract λ_c by equating the analytical solution to the measured susceptibility of the A-needle. Figure 5 depicts the calculated $\lambda_{ab}(T)$ and $\lambda_c(T)$ for $x = 7\%$. Two arrows show the temperature where H_{c1} is on the order of our measurement field (0.5 Oe). Eq. 1 is valid at temperatures lower than indicated by the arrows. It is also clear that the magnetization is finite when the penetration depth reaches the sample's dimensions.

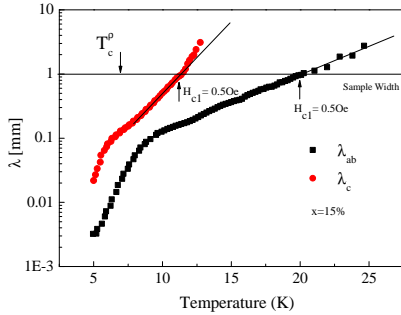


FIG. 5: A semi log plot of the penetration depths λ_{ab} and λ_c , for the 7% sample, as a function of T obtained by comparing the analytical solutions of Eq. 1 and 2 with the measured susceptibilities. The horizontal line represents the sample width. The points at which H_{c1} , for each needle, equals the applied field are also shown by arrows.

The surprising result is that λ_{ab} and λ_c run away from each other as the sample is warmed beyond T_c^p , and both reach the sample dimensions well above T_c^p . This means that if we could increase the thickness of our samples, while maintaining needle-like geometry, we would expect only larger difference between the temperature of zero magnetization and T_c^p , in contrast to a finite size scenario.

It is important to mention that there are other experimental works showing a strong anisotropy in the tem-

perature at which signals can be picked in LSCO [9]. In addition, it was recently suggested theoretically that two dimensional like superconductivity could be generated by frustration in the inter-layer coupling caused by stripes [10], or by c-axis disorder [11]. This could lead to two different magnetic critical temperatures.

To summarize, in this work we examined the anisotropy in the susceptibility of $\text{La}_{2-x}\text{Sr}_x\text{CuO}_4$ single crystals cut as needles. Our major findings are: I) diamagnetic susceptibility above T_c^p for $H \parallel c$ at all doping, and in the zero field limit, II) diamagnetic susceptibility above T_c^p for both $H \parallel c$ and $H \perp c$ at low doping. We suggest that at low doping, electronic inhomogeneous localization is leading to local 3D superconducting patches, which provide diamagnetism without global superconductivity.

-
- [1] N. D. Mermin and H. Wagner, Phys. Rev. Lett. **17**, 1133 (1966).
 - [2] Y. Wang, L. Li, M. J. Naughton, G. D. Gu, S. Uchida, and N. P. Ong, Phys. Rev. Lett. **95**, 247002 (2005); Lu Li, Yayu Wang, M. J. Naughton, S. Ono, Yoichi Ando, and N. P. Ong, Europhys. Lett. **72**, 451-457 (2005); Lu Li, Yayu Wang, Seiki Komiya, Shimpei Ono, Yoichi Ando, G. D. Gu and N. P. Ong, Phys. Rev. B **81**, 054510 (2010).
 - [3] G. S. Boebinger *et al.*, PRL **77**, 5417 (1996); J. Hori, S. Iwata, H. Kurisaki, F. Nakanura, T. Suzuki, and T. Fuhita, J. Phys. Soc. Jpn. **71** (2002) 1346; S. Komiya and Y. Ando, PRB **70** (2004) 060503(R).
 - [4] S. Komiya, Y. Ando, X. F. Sun, and A. N. Lavtsov, Phys. Rev. B **65**, 214535 (2002). Y. Ando, S. Komiya, K. Segawa, S. Ono, and Y. Kurita, Phys. Rev. Lett. **93**, 267001 (2004).
 - [5] M. Sato and Y. Ishii J. Appl. Phys. **66**, 983 (1989).
 - [6] D. Feinberg *et al.*, Phys. Rev. Lett. **65**, 919 (1990); V. Vulcanescu *et al.*, Phys. Rev. B **50** 4139 (1994); P.A. Mansky *et al.*, Phys. Rev. B **52** 7554 (1995); Yu.V. Bugoslavsky *et al.*, Phys. Rev. B **56**, 5610 (1997); Y. Bruckental *et al.*, Phys. Rev. B **73**, 214504 (2006).
 - [7] C. Panagopoulos *et al.*, Phys. Rev. B **53**, R2999 (1996); A. Gardchareon, N. Mangkorntong, D. Hérisson, P. Nordblad, Physica C **439**, 85 (2006).
 - [8] Polyanin A D, 2002 Handbook of Linear Partial Differential Equations for Engineers and Scientists (London: Chapman and Hall).
 - [9] Q. Li, M. Hucker, G.D. Gu, A. M. Tsvelik, J. M. Tranquada, Phys. Rev. Lett. **99**, 067001 (2007); A. A. Schafgans, A. D. LaForge, S. V. Dordevic, M. M. Qazilbash, W. J. Padilla, K. S. Burch, Z. Q. Li, Seiki Komiya, Yoichi Ando, and D. N. Basov, Phys. Rev. Lett., **104**, 157002 (2010).
 - [10] E. Berg *et al.*, Phys. Rev. Lett. **99**, 127033 (2007).
 - [11] P. Mohan, P. M. Goldbart, R. Naryanan, J. Toner, and T. Vojta, Phys. Rev. Lett **105**, 085301 (2010); D. Pekker, G. Refael, and E. Demler, Phys. Rev. Lett. **105**, 085302 (2010).

SUPPLEMENTARY MATERIAL

To test the doping homogeneity of the grown crystal we cut the 7% A-needle to 5 pieces, grained them into powder to remove shape dependent effects, and measured the magnetization of each piece. The data is presented in Fig. 1. Juggling from the scatter of points at half of the full magnetization, there is a scatter in T_c of 2 K between the different pieces. This is much smaller than the difference between all other critical temperatures.

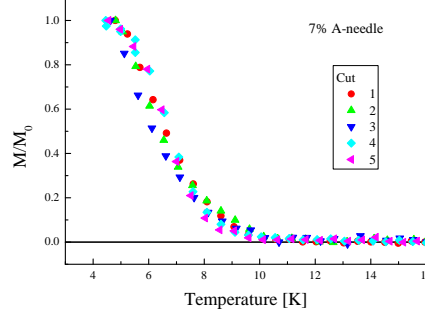


FIG. 1: Magnetization as a function of temperature measurements performed on 5 different pieces cuts from the 7% A-needle. The pieces were ground into powder.

We also measured H_{c1} for the other three samples. In Fig. 2 we depict H_{c1} as a function of temperature. As long as the data does not cross $H = 0.5$ Oe upon warming, there are no vortices in the sample.

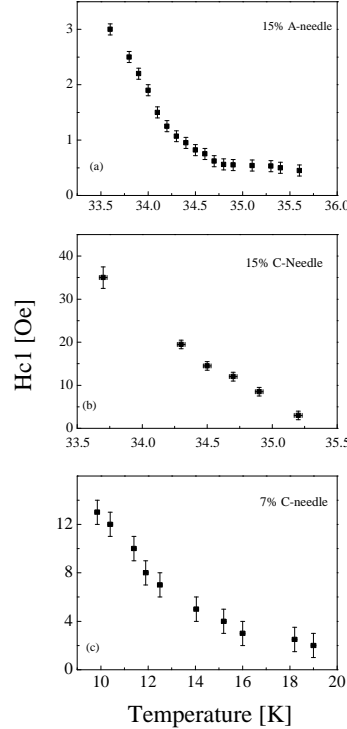


FIG. 2: H_{c1} as a function of temperature measured on (a) 15% A-needle (b) 15% C-needle (c) 7% C-needle.

In Fig. 3 we provide the field dependence of the susceptibility for the 7% needles. The susceptibility converges in to a field independent function at $H \rightarrow 0$, especially close to T_c . In the inset we show tilt experiment for the 7% needles.

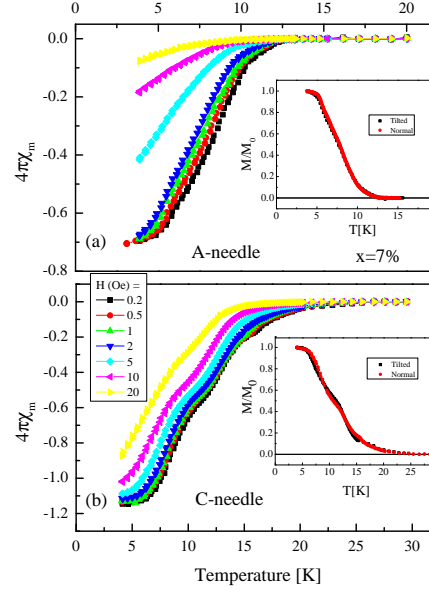


FIG. 3: The measured susceptibility χ_m ($\equiv M/H$) as a function of temperature for the 7% (a) C-needle and (b) A-needle in various magnetic fields. Insets: measurements of a straight and tilted needles demonstrating the effect of misalignment.

We also performed shape dependent measurements for the 7% samples. They are presented in Fig. 4. However, the 7% sample are not ideal to test the impact of geometry on the magnetization. Each one of the samples presented in the figure is cut from a different place along the rod, which are away from each other by few centimeters. Since around 7% doping T_c is hyper-sensitive to doping variations, the different samples could have T_c variation of ~ 2 K. Consequently, in Fig. 4 not only the geometry varies. This is not the case for 15% sample in which T_c is not sensitive to doping variations.

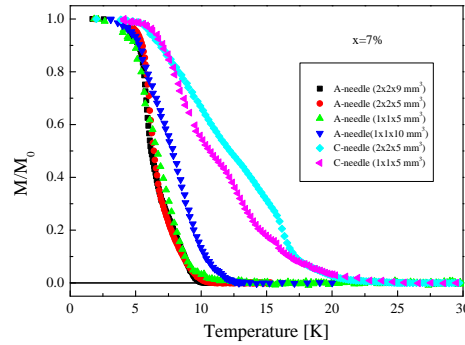


FIG. 4: Magnetization versus temperature for several 7% A- and C-needles with different sample dimensions.